JPE 7-4-3

Proposed Distribution Voltage Control Method for Connected Cluster PV Systems

Kyung-soo Lee[†], Kenichiro Yamaguchi[*] and Kosuke Kurokawa[*]

[†*]Dept. of Electronics and Information Eng., Tokyo University of Agriculture and Technology, Tokyo, Japan

ABSTRACT

This paper proposes a distribution voltage control method when a voltage increase condition occurs due to reverse power flow from the clustered photovoltaic (PV) system. This proposed distribution voltage control is performed a by distribution-unified power flow controller (D-UPFC). D-UPFC consists of a bi-directional ac-ac converter and transformer. It does not use any energy storage component or rectifier circuit, but it directly converts ac to ac. The distribution model and D-UPFC voltage control using the ATP-EMTP program were simulated and the results show the voltage increase control in the distribution system.

Keywords: reverse power flow, clustered photovoltaic system, distribution-unified power flow controller, bi-directional ac-ac converter, ATP-EMTP

1. Introduction

In present power systems, the generated power is assumed to feed into the system at a high voltage level and the power is consumed at a low voltage level. Thus, the power direction through a transformer would always be from the high voltage level to the low voltage level[1].

However, if the distributed generation (DG) like PV system connects with the grid, the reverse power flow can occur. When the reverse power flows from the PV side to the grid, the PV side voltage level is higher than the grid side. When a clustered PV system, and not a PV system, connects with the grid, a voltage increase condition occurs. The voltage curve of the clustered PV system with the grid is shown in Fig. 2.

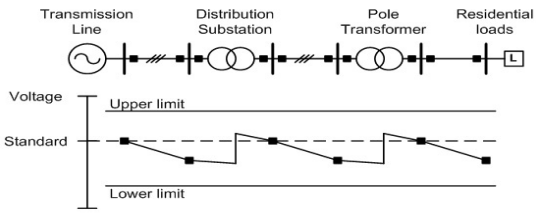

Fig. 1 Voltage curve of the present power system

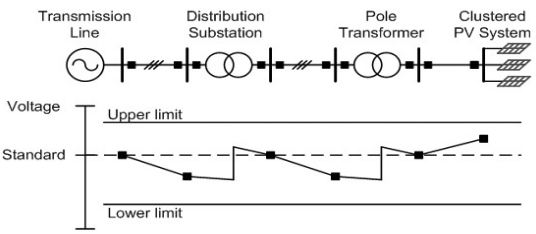

Fig. 2 Voltage curve of the clustered PV system connected with grid

Manuscript received ; April 23, 2007; revised July 24, 2007
[†]Corresponding Author: onnuri@cc.tuat.ac.jp
Tel : +81-042-388-7445, Tokyo Univ. of Agriculture and Technology
[*]Dept. of Electronics and Information Eng., Tokyo Univ. of Agriculture and Technology

So far, voltage control methods of the distribution system during voltage decrease and voltage increase have been researched. In the grid side voltage control methods, a static var compensator (SVC) has been used by controlling reactive power. However, the reactive control makes power loss in the distribution system. Line drop compensator (LDC) and scheduled voltage operation methods have been performed controlling substation voltage tap. But, it is known that it can not rapidly control the distribution voltage when voltage variation occurs. Also, a dynamic voltage restorer (DVR) has been used in the grid system. However, it depends on the capacitor size. If the power increases, the capacitor size will increase [2]. Autotransformer based step voltage regulator (SVR) has been used but it takes 100[ms] to several seconds to control the voltage.

Also, PV side voltage control methods, which solve mainly voltage increase conditions, have been developed. The first method is to restrict the PV output power when the distribution voltage reaches the over-voltage limit. For the second method, the reactive power control from the PV inverter can avoid the over-voltage limit. Finally, the PV inverter with battery system can assist to prevent over-voltage conditions in the distribution system. Grid and PV side voltage control methods are summarized in Table 1.

Table 1 Summary of grid and PV side voltage control methods

Grid side voltage control methods
Reactive power control – SVC
Substation control - LDC, Scheduled operation
Voltage tap control – SVR
PV side voltage control methods
Power restriction control - PV output power restriction
Reactive power control - PV output power factor change
Battery control - PV output power to battery charge

Here, the proposed D-UPFC is the grid side voltage controller. D-UPFC has advantages compared with other grid side voltage controllers. For example, it controls the distribution voltage during forward power flow and reverse power flow. It controls the distribution voltage within several cycles. It has linear voltage characteristics when the converter is performed because of PWM control.

This paper begins by studying D-UPFC topology. Voltage control method and switching pattern of bi-directional ac-ac converter are analyzed. In the transformer, transformer power rating calculation is studied. Distribution model is simulated using the ATP-EMTP program. Finally, D-UPFC is injected into the distribution model in order to verify voltage increase control in the distribution system.

2. D-UPFC Analysis

2.1 Bi-directional ac-ac converter topology

The bi-directional ac-ac converter consists of four MOSFET switches and input & output LC filters. The converter topology is shown in Fig. 3.

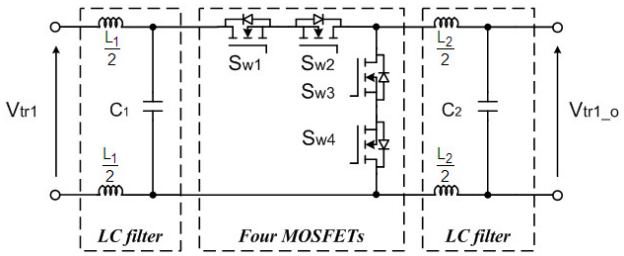

Fig. 3 Bi-directional ac-ac converter topology

Input and output voltage relation of the converter is the same as the dc-dc buck converter [3]. Thus, the ac-ac converter voltage equation can be expressed,

$$V_{tr1\_o} = DV_{tr1} \tag{1}$$

where, D is duty ratio of the ac-ac converter.

2.2 Converter control

In the bi-directional ac-ac converter control, the reference signal to inject PWM should be used after transforming the dc signal. So far, one of methods uses single phase direct-quadrature (d-q) transformation [4]. Its main advantage is that it can control the transient response quickly. The other option is to use root-mean-square (RMS) function. It is easy to design both in simulation and experiment. Here, the ac-ac converter uses rms function in the simulation. Bi-directional ac-ac converter control method is shown in Fig. 4.

In the control method, ac-ac converter output voltage V_{tr1_o} is injected into RMS function and then it is transformed to dc signal. The reference dc voltage V_{ref} compares with $V_{tr1\_o\_dc}$. The value of V_{error} is used through PI and PWM controls. Finally, the switching patterns from S_{w1} to S_{w4} are decided by phase detect function with logic circuit.

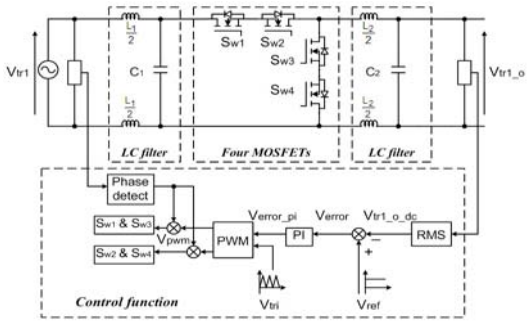

Fig. 4 Bi-directional ac-ac converter control method

2.3 Converter switching patterns

The switching patterns in the bi-directional ac-ac converter offer safe commutation without high-voltage spikes using intelligent PWM switching patterns. Also, the switching patterns are decided by the polarity of the input voltage V_{tr1}. Figure 5 to 7 shows the switching patterns during forward power flow condition and the input voltage V_{tr1} is positive. When V_{tr1} is positive, S_{w1} and S_{w3} act PWM switching reversely. At the same time, S_{w2} and S_{w4} turn on. If the sign of the V_{tr1} is changed, the switching patterns are reversed. In the switching patterns, active, dead-time and freewheeling modes are divided by converter operation. In the active mode, $S_{w1,3}$ perform PWM and $S_{w2,4}$ turn on as shown in Fig. 5. Thus, the inductor current flows through input voltage. The dead-time mode occurs during $Sw_{1,3}$ as they turn off together. The current paths can be formed by the direction of the inductor current as shown in Fig. 6. In the freewheeling mode as shown in Fig. 7, the output filter inductor current flows to the load through switch $S_{w3,4}$[5].

Figure 8 to 10 shows the switching patterns when reverse power flows from clustered PV system to the grid. The clustered PV system is regarded as the current source. Switching patterns from Fig. 8 to 10 are the same as Fig. 5 to 7 because the sign of V_{tr1} is the same. If the sign of V_{tr1} is changed, the switching patterns are also reversed.

Switching patterns of the ac-ac converter from Fig. 5 to 10 can be created using a logic circuit as shown in Fig. 11. This logic circuit of bi-directional ac-ac converter is performed in the simulation.

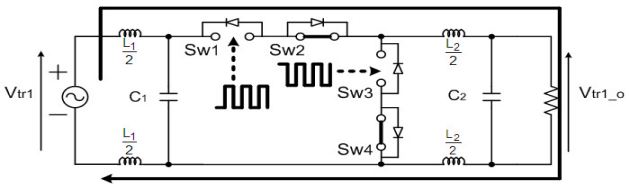

Fig. 5 Active mode during forward power flow

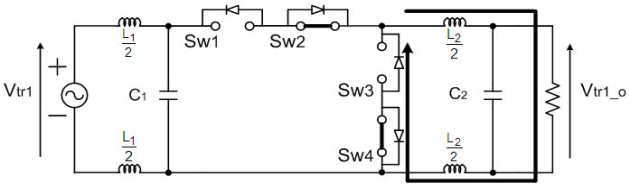

Fig. 6 Dead-time mode during forward power flow

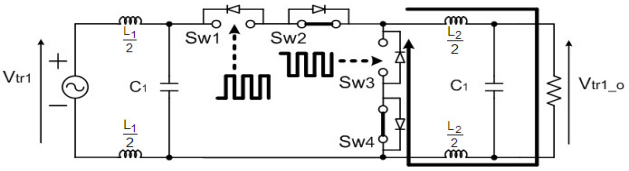

Fig. 7 Freewheeling mode during forward power flow

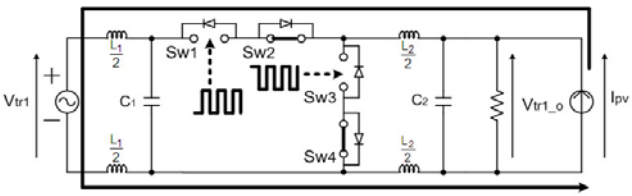

Fig. 8 Active mode during reverse power flow

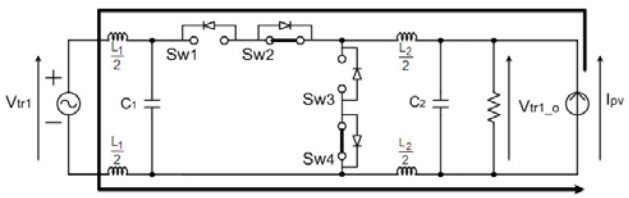

Fig. 9 Dead-time mode during reverse power flow

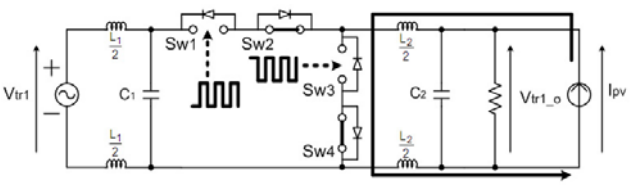

Fig. 10 Freewheeling mode during reverse power flow

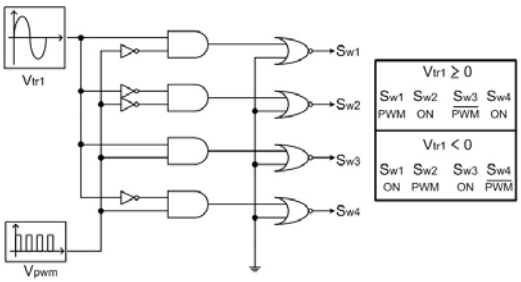

Fig. 11 Logic circuit of the converter switching pattern

2.4 Transformer power rating and D-UPFC voltage control

The transformer is an essential component to design D-UPFC topology. In the D-UPFC voltage control, the transformer mainly takes charge of the input voltage in the distribution system. D-UPFC topology is shown in Fig. 12.

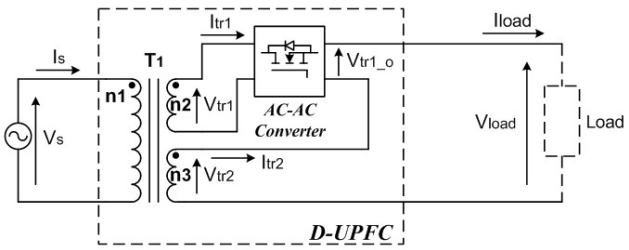

Fig. 12 D-UPFC topology

D-UPFC consists of T_1, which is transformer, and ac-ac converter. The primary side of T_1 is connected with secondary voltage V_s of the pole transformer. The secondary side of T_1 is divided two transformers and the upper transformer is connected with ac-ac converter and the lower transformer supplies a part of constant voltage to the converter[6].

In order to calculate the power rating of T_1, the value of turns ratio n_1, n_2 and n_3 are assumed to 1, 0.2 and 0.9, respectively. Considering the power rating of T_1,

$$P_s = V_s I_s \tag{2}$$

$$P_{tr1} = V_{tr1} I_{tr1} \tag{3}$$

$$P_{tr2} = V_{tr2} I_{tr2} \tag{4}$$

Total power of T_1 is,

$$P_s = P_{tr1} + P_{tr2} \tag{5}$$

$$V_s I_s = \frac{1}{5} V_{tr1} I_{tr1} + \frac{9}{10} V_{tr2} I_{tr2} \tag{6}$$

AC-AC converter input current I_{tr1} is decided by,

$$I_{tr1} = D I_{tr2} \tag{7}$$

If duty ratio D of ac-ac converter is 0.5 during normal condition, the equation (6) can be rewritten as,

$$V_s I_s = \frac{1}{10} V_{tr1} I_{tr2} + \frac{9}{10} V_{tr2} I_{tr2} \tag{8}$$

If the value of load is decided,

$$I_s = I_{tr2} = I_{load} \tag{9}$$

Finally, equation (8) can be rewritten as,

$$V_s I_s = \frac{1}{10} V_{tr1} I_s + \frac{9}{10} V_{tr2} I_s \tag{10}$$

If the transformer is ideal, the transformer power rating can be calculated by equation (10). The relationship of the value of n_2, n_3 can be shown in Fig. 13.

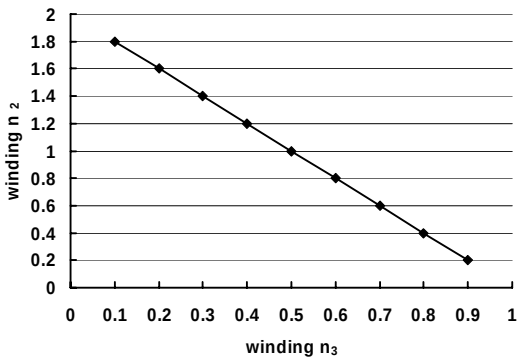

Fig. 13 Transformer power rating calculated by n_2 and n_3

In the D-UPFC voltage control from Fig. 12, the load voltage is decided,

$$V_{load} = V_{tr1\_o} + V_{tr2} \tag{11}$$

where, V_{tr1_o} is output voltage of ac-ac converter and V_{tr2} is output voltage of the secondary of T_1.

$$V_{tr1\_o} = \frac{1}{5} V_s D \tag{12}$$

$$V_{tr2} = \frac{9}{10} V_s \tag{13}$$

where, n_1:n_2:n_3 = 1:0.2:0.9.

The goal of D-UPFC voltage control is,

$$V_{load} = V_{ref} \tag{14}$$

where, V_{ref} is the reference voltage. It is assumed 202[V,rms] which is the pole transformer secondary voltage.

If the increasing voltage condition occurs due to reverse power flow from the clustered PV system, the load voltage increases as,

$$V_{load} = (1+n) V_{ref} \tag{15}$$

where, n means the increasing voltage per unit.

Rewrite from equation (11) to (15),

$$(\frac{1}{5} V_s D) + (\frac{9}{10} V_s) = (1+n) V_{ref} \tag{16}$$

In the end, ac-ac converter duty ratio D is calculated as,

$$D = \frac{(1+n) V_{ref}}{\frac{1}{5} V_s} - \frac{9}{2} \tag{17}$$

3. D-UPFC Simulation Results

In this section, the distribution model is simulated. In order to verify D-UPFC voltage control during increased voltage conditions, D-UPFC is injected to the distribution model.

3.1 Distribution model

The distribution model using ATP-EMTP program is shown in Fig. 14. The distribution model is assumed to be a residential area in Japan. Total feeders of the distribution model are eight. The length of one feeder is 10[km] and the pole tranformer is located every 2[km]. Each pole transformer connects with 20 houses and divided by 4 nodes. The distance between node A_{21} and A_{22} is 40[m]. Each 5 houses connect with the node from A_{21} to A_{24} in parallel. The distance between node to each house is 15[m]. The capacity of each PV output power is 3[kW]. Distribution model parameters are shown in table 2.

Table 2 Distribution model parameters

Substation		66kV/6.6kV, 20MVA
Pole transformer		6.6kV/202V(101V), 50kVA
HV line impedance(Z_1toZ_5)		0.626+j0.754[Ω/2km]
LV line impedance($Z_{d1}$to Z_{d3})		0.025+j0.020[Ω/40m]
Lead-in wire imp.(Z_{i1}toZ_{i20})		0.0552+j0.037[Ω/20m]
Total load	Light load	4.08[Ω]
	Heavy load	1.02[Ω]
Each PV source(1 to 20)		3[kW]

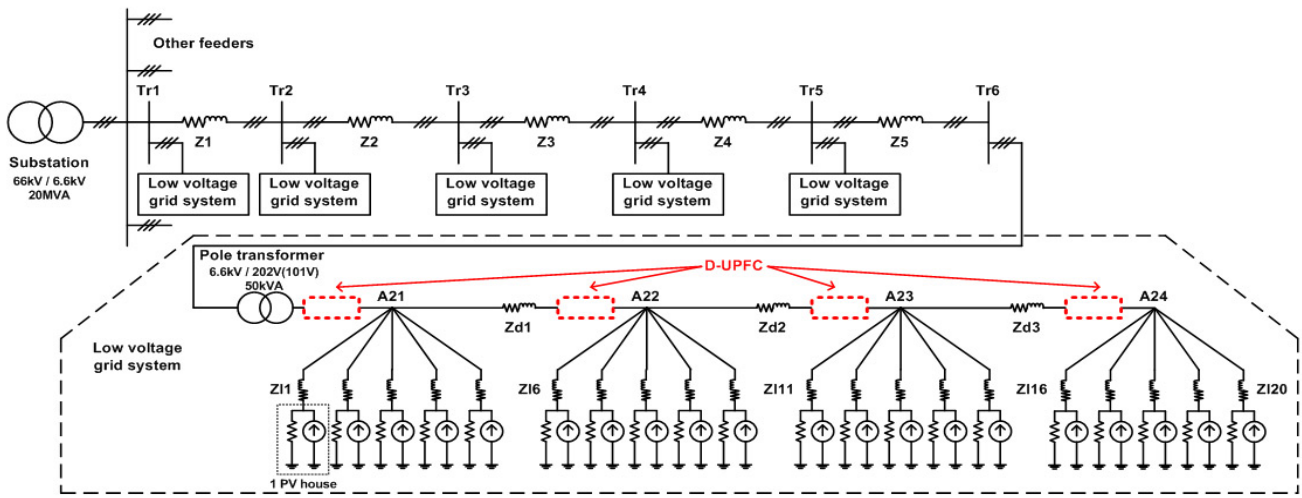

Fig. 14 Distribution model in the ATP-EMTP simulation

There are three constraints in the simulation:

(1) Each feeder is radial topology.

(2) Loads only consist of resistance.

(3) PV output power factor is 1.

3.2 Distribution model simulation results

The pole transformer secondary voltage range is 202±20(101±6) [V,rms]. In the light load condition, total power is consumed 20[%] of the pole transformer power rating. 80[%] of the pole transformer power is consumed during heavy load situation. In the reverse power flow condition, 20 PV systems from node A_{21} to A_{24} connect with pole transformer. Each PV system generates 3[kW] and thus, it totally generates 60[kW]. From clustered PV power supply 10[kW] for the load and remained about 50[kW] flows to the pole transformer.

It means that the reverse power flows to the pole transformer side with maximum power capacity of the pole transformer.

The voltage curves during light load, heavy load, and light load with reverse power flow are shown in Fig. 15. In the light load condition, the pole transformer secondary voltage decreased 100.55[V,rms] at node A_{21} to 99.65[V,rms] at node A_{24}. In the heavy load condition, the voltage decreased 99.3[V,rms] at node A_{21} to 95.75[V,rms] at node A_{24}. In the light load with reverse power flow condition, the voltage increased 101.45[V,rms] at node A_{21} to 106.15[V,rms] at node A_{24}. Here, the A_{21} voltage is not the same as pole transformer reference voltage 101[V,rms] because the clustered PV system with loads are located in T_{r6}, which is 10[km] far from the substation.

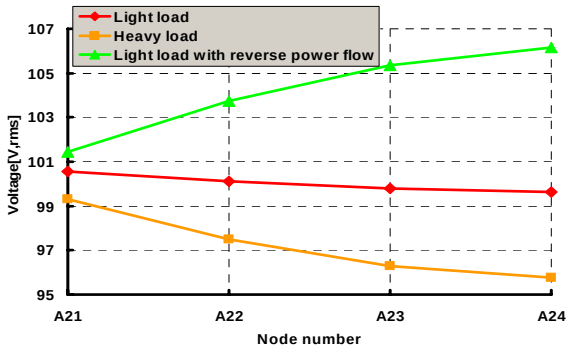

Fig. 15 Voltage curves at the pole transformer secondary side

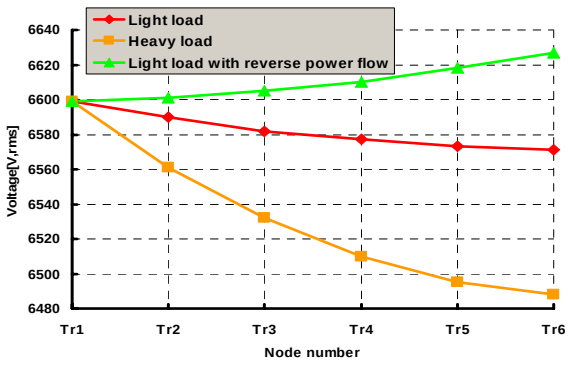

Fig. 16 Voltage curves at the pole transformer primary side

The pole transformer primary side voltage curves are also drawn during light load, heavy load, and light load with reverse power flow conditions which is shown in Fig. 16. Similar with the pole transformer secondary side voltage, the voltage decreased during light and heavy load. In the light load with reverse power flow condition, the voltage increased 6600[V,rms] at T_{r1} to 6627[V,rms] at T_{r6}.

In the reverse power flow simulation, D-UPFC is injected to the distribution model. D-UPFC parameters are shown in table. 3.

Table 3 D-UPFC parameters.

V_S	202[V,rms]	C_1 & C_2	50[μF]
n_1:n_2:n_3	1:0.2:0.9	V_{ref}	202[V,rms]
V_{tr1}	40.4[V,rms]	K gain of P	0.025
V_{tr2}	181.8[V,rms]	K gain of I	0.001
L_1 & L_2	50[μH]	Switching freq.	20[kHz]

The reverse current increased 250[A,rms] from 0.02[s] to 0.1[s]. Figure 17 shows the reverse current waveform from the clustered PV system.

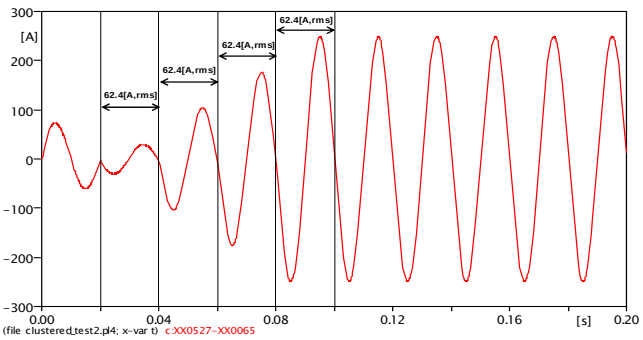

Fig. 17 Reverse current flow from the clustered PV system

Figure 18 shows D-UPFC voltage waveforms during voltage increase condition. V_{tr2} is 181.8[V,rms] and ac-ac converter input voltage V_{tr1} is 40.4[V,rms]. V_{tr1_o} is decided by D-UPFC control. V_{tr1} and V_{tr1_o} of the bi-directional ac-ac converter are close to the same phase angle and thus, it does not generate reactive power to control the distribution voltage in the ac conversion.

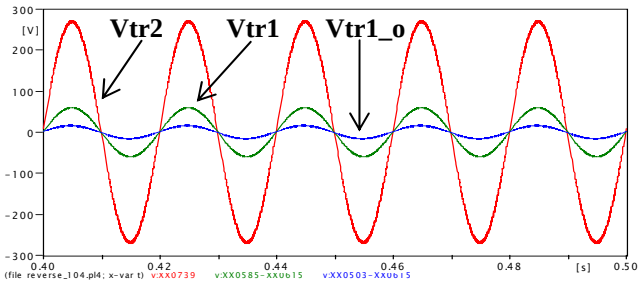

Fig. 18 D-UPFC voltage waveforms during voltage increase control at node A_{24}

Fig. 19 shows the simulation results of D-UPFC voltage control in the distribution model. As mentioned from Fig. 15, the pole transformer secondary voltage increased from 101.45[V,rms] at node A_{21} to 106.15[V,rms] at node A_{24} during reverse power flow condition. D-UPFC is injected into node A_{21} to A_{24}. In the D-UPFC voltage control, the reference voltage is 101[V,rms], which is the pole transformer secondary voltage. When D-UPFC controls the distribution voltage at node A_{21}, the controlled voltage is 101.7 [V,rms]. The controlled voltage is affected from the reverse power of the PV system thus, it does not follow the reference voltage 101[V,rms]. D-UPFC controls the distribution voltage to 101.7[V,rms] at node A_{22} and 101.25[V,rms] at node A_{23}. In the node A_{24}, D-UPFC controls the voltage to 100.95[V,rms].

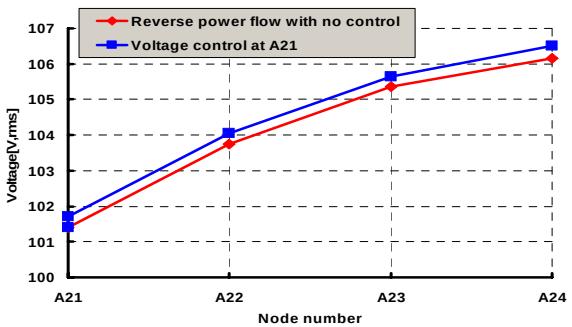

(a) D-UPFC installation at node A_{21}.

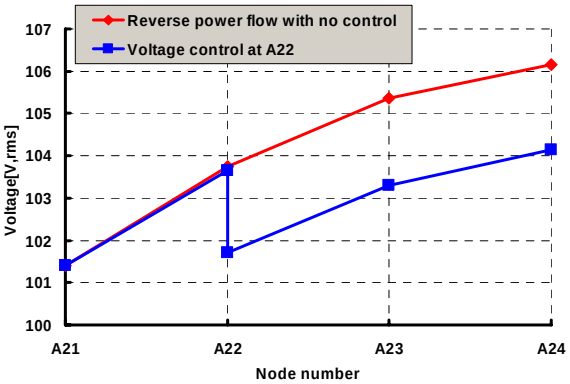

(b) D-UPFC installation at node A_{22}.

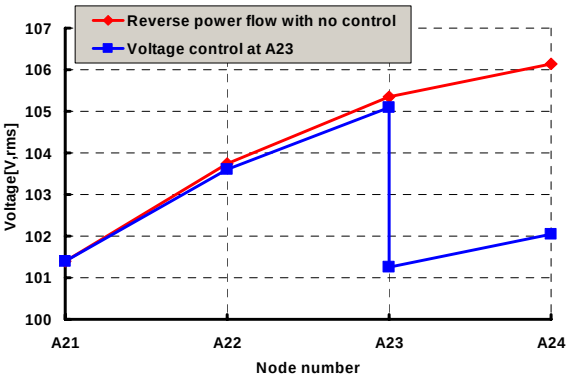

(c) D-UPFC installation at node A_{23}.

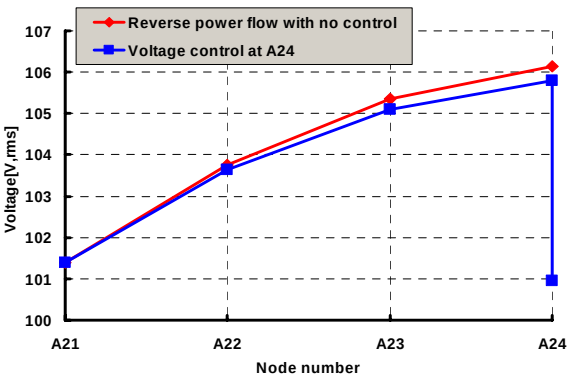

(d) D-UPFC installation at node A_{24}.

Fig. 19 D-UPFC voltage control in the distribution model during reverse power flow condition

Through the D-UPFC control simulation, D-UPFC only controls the distribution voltage at the installation area and it has a voltage control limit due to the distance.

4. Conclusions

Distribution model and D-UPFC using ATP-EMTP program for controlling voltage increase condition are simulated in this paper. D-UPFC consists of bi-directional ac-ac converter and transformer. The converter topology, control method and switching patterns are shown.

Transformer power rating calculation is performed. Distribution model simulations show the voltage curves during load and reverse power flow conditions. D-UPFC partially controls the voltage increase when it is installed for each node.

Acknowledgment

This research has been carried as a part of "Autonomy-Enhanced PV Cluster" project and thanks for financial support of NEDO. The author offers special thanks to Prof. Koizumi and Prof. Ohashi for their comments on this research.

References

[1] A. F. Povlsen, "Impacts of Power Penetration from Photovoltaic Power Systems in the Distribution Networks", IEA PVPS T5-10, pp. 2~5, Feb. 2002.

[2] J. Pérez, V. Cárdenas, H. Míranda, and R. Álvarez, "Compensation of Voltage Sags and Swells using a Single-phase AC-AC Converter", The 30th Annual Conference of the IEEE Industrial Electonics Society, pp. 1611~1616, Nov. 2004.

[3] K. S. Lee, K. Yamaguchi, H. Koizumi, and K. Kurokawa, "D-UPFC as a Voltage Regulator in the Distribution System", Renewable Energy 2006, pp. 1756~1759, Oct. 2006.

[4] R. Zhang, M. Cardinal, P. Szczesny, M. Dame, "A Grid Simulator with Control of Single-Phase Power Converters in D-Q Rotating Frame", IEEE PESC'02, pp. 1431~1436, June 2002.

[5] B. Kwon, B. Min, and J. Kim, "Novel topologies of AC choppers", IEE Proc. Electr. Power Appl., Vol. 143, No. 4, pp. 323~330, July 1996.

[6] E. C Aeloíza, P. N. Enjeti, L. A. Morán, O. C. Montero-Hernandez, and S. Kim, "Analysis and Design of a New Voltage Sag Compensator for Critical Loads in Electrical Power Distribution Systems," IEEE Trans. Ind. Appli., Vol 39, No. 4, pp. 1143-1150, July/Aug. 2003.

Kyung-Soo Lee was born in Buan, Korea, in 1978. He received B.E. from Hoseo University, Korea in 2003 and M.E. from Chungbuk National University, Korea in 2005. Now he is a doctoral course student in the Department of Electronic and Information Engineering, Tokyo University of Agriculture and Technology. His main areas of interests are power electronics applied to power systems including grid-connected PV inverter, ac-ac converter, and power quality issue. Mr. Lee is a student member of IEEJ, IEEE.

Kenichiro Yamaguchi was born in Nagasaki, Japan, in 1984. He received his B.E. from Tokyo University of Agriculture and Technology, Japan in 2007. Now he is a Master's course student in Department of Electrical and Electronic Engineering, Tokyo University of Agriculture and Technology. His main areas of interests are power electronics including ac-ac converter.

Kosuke Kurokawa is currently with Electrical and Electronic Engineering Department, Faculty of Technology, Tokyo University of Agriculture and Technology. After graduation from Waseda University in 1965, he joined Electro-technical Laboratory, Ministry of International Trade and Industry and has been engaged in research on energy systems technology for 30 years mainly at Electro-technical Laboratory. He received his Doctorate Degree of Engineering from Waseda University in 1993. He moved to his present position in May 1996. His current research interests include Solar Energy, Photovoltaic Systems Engineering and Energy Systems Analysis. He has been the Operating Agent of Task VIII in photovoltaic system R&D program by the International Energy Agency since 1998. He was assigned the General Chairperson of the 3rd World Conference in Osaka, May 2003. He was also assigned the General Chairperson of the Renewable Energy 2006 in Chiba, October 2006.